

TXNIP Participated in NLRP3-Mediated Inflammation in a Rat Model of Cervical Spondylotic Myelopathy

Peisheng Liu^{1,*}, Xiaofeng Li^{1,*}, Jing Liu², Hengjia Zhang¹, Zhitao You¹, Jianfeng Zhang¹ 

¹Department of Spinal Surgery, Yantaishan Hospital, Yantai, People's Republic of China; ²Basic Department, Yantai Vocational College, Yantai, People's Republic of China

*These authors contributed equally to this work

Correspondence: Jianfeng Zhang, Department of Spinal Surgery, Yantaishan Hospital, No. 10087, Keji Avenue, Laishan District, Yantai, People's Republic of China, Tel +86-13780921732, Email zhangjifdoctor@126.com

Background: Cervical spondylotic myelopathy (CSM) is a spinal cord disease caused by cervical disc degeneration and related pathological changes. Cervical spondylotic myelopathy may result from inflammation responses and neuronal damage. Thioredoxin-interacting protein (TXNIP)/NOD-like receptor protein 3 (NLRP3) signaling promotes inflammation. However, the effects of TXNIP/NLRP3 on the pathogenesis of CSM have not been reported.

Methods: A rat model of chronic cervical cord compression was established to observe changes in the levels of TXNIP/NeuN and NLRP3/NeuN expression in the damaged anterior horn of the spinal cord following progression of CSM. Rats were injected with TXNIP small interfering RNA (siRNA) and scrambled control to determine the effects of TXNIP inhibition on NLRP3-mediated inflammation in rats with CSM. Behavioral effects and the expression of NLRP3 and pro-caspase-1 in the damaged spinal cord were evaluated.

Results: The expression levels of TXNIP and NLRP3 were significantly increased in the damaged anterior horn of the spinal cord following CSM. Injection of TXNIP siRNA significantly improved behavioral measures and decreased apoptosis in the damaged anterior horn of spinal cord. Furthermore, the levels of NLRP3 and pro-caspase-1 in the lesioned area were reduced by the TXNIP siRNA injection.

Conclusion: Thioredoxin-interacting protein participated in NLRP3 mediated inflammation in a rat model of CSM, which indicated that TXNIP may be a potential therapeutic target in improving CSM.

Keywords: neuroinflammation, TXNIP/NLRP3, spinal cord dysfunction, pro-caspase-1

Introduction

Cervical spondylotic myelopathy (CSM) is a spinal cord disease caused by cervical disc degeneration and related pathological changes. It is the most common form of spinal cord injury in adults, accounting for about 5–10% of cervical spondylosis.^{1,2} Cervical spondylotic myelopathy can result in long-term disability and major neurological impairments. However, exact pathophysiology underlying CSM has not been characterized. Neuronal loss, axonal injury and neuroinflammation have been observed in cases of CSM and in several experimental animal models.^{3–6} Among these mechanisms, neuroinflammation could induce glial cell activation, resulting in aggravation of existing damage and worsening of the damage-associated microenvironment. Therefore, persistent neuroinflammation plays a crucial role in the complex pathology of CSM.

Neuroinflammation can cause secondary injuries, resulting in neuronal death.⁷ Several studies have shown that inflammation can extend to adjacent tissues, triggering cell death and inhibition of axonal regeneration and restoration of function after spinal cord injury.^{8–10} Recent studies have shown that activation of the inflammasome pathway

stimulates secretion of pro-inflammatory factors to initiate cell death.^{11,12} Inflammasomes typically contain NOD-like receptor protein 3 (NLRP3), apoptosis-associated speck-like protein containing a caspase recruitment domain (ASC) and pro-caspase-1, which associate after various endogenous risk signals.¹² Activation of NLRP3 mediates recruitment of pro-caspase-1 and promotes secretion of pro-interleukin (IL)-1 β and pro-IL-18. Targeting the NLRP3 inflammasome could promote neuroprotection in injured spinal cord.¹³ In a rat model of CSM, the NLRP3 inflammasome was activated.^{1,4} However, the mechanisms by which the NLRP3 inflammasome activated in CSM are unclear.

Thioredoxin-interacting protein (TXNIP) is a crucial molecular sensor of oxidative stress and inflammation that plays in regulation of energy metabolism. Thioredoxin-interacting protein was identified as a potential binding partner of NLRP3 in a yeast two hybrid system. Leucine-rich repeats (LRR) in TXNIP can bind to the NLRP3 inflammasome in various diseases.^{14,15} In response to oxidative stress, TXNIP is released from oxidized thioredoxin (TRX) and binds to the NLRP3 inflammasome, resulting in pyroptosis through secretion of IL-1 β and IL-18.¹⁵ Pyroptosis is a form of programmed cell death with an inflammatory component.¹⁶ The inflammasome sensor NLRP3 is effector of pyroptosis, and can be activated by extracellular or intracellular stimulation. The TXNIP/NLRP3 pathway has been studied in spinal cord injury-related diseases.^{17–19} High expression of TXNIP induced activation of the NLRP3 inflammasome in injured spinal cords and triggered pyroptosis.¹⁹ Inhibition of this has potential to improve recovery from spinal cord injury. However, the role of TXNIP in CSM has not been reported, and the role of the TXNIP-NLRP3 interaction has also not been characterized in CSM. These findings indicated that TXNIP/NLRP3 may be a potential target for treatment of CSM.

In this study, a rat model of CSM was established, and the expression levels of TXNIP and NLRP3 were quantitated in the anterior horn of the spinal cord following CSM. We suppressed TXNIP expression using small interfering RNA (siRNA) to observe the effects of TXNIP on the NLRP3 inflammation in the CSM. We hypothesized that TXNIP triggers activation of NLRP3 in CSM, and that inhibition of TXNIP could reduce CSM-induced neuroinflammation.

Materials and Methods

Animals

Adult Sprague Dawley rats, male and female, weighting 300–400g, were purchased from Jinan Pengyue Experimental Animal Breeding Co., Ltd (Jinan, Shandong, China). Eighty-five rats ear-tagged with numerical identifiers were housed under a 12 h light/dark cycle maintained at 20–24°C, 40–70% relative humidity, and were allowed free access to food and water. All experimental protocols were approved by the Animal Care Committee of the Yantaishan Hospital (Number: 2,021,002), and followed the Guide for the Care and Use of Laboratory Animals published by the US National Institutes of Health (2011).

Chronic Cervical Cord Compression Model

According to previous methods,^{1,5,20} the rats were anesthetized with an intraperitoneal injection of pentobarbital (40 mg/kg). A midline incision was made at the cervical area (C2–T2), and the skin and superficial muscles were retracted. The rats underwent a C5–C6 laminectomy, and a chronic progressive compression device was inserted into the C5–C6. The compression device was a plexiglass flat plate (10 mm \times 6 mm), with a 2 mm diameter screw hole in the center and a 1-mm diameter round hole at each corner (JiTian Bio, Beijing, China). Suture was tied and fixed to the interspinous ligament and sacral spinal muscle tendon, then threaded through the small holes around the plate to tie and fix the compression device. A screw with pitch of 0.4 mm, length of 10 mm and diameter of 2 mm was advanced exactly 0.2 mm (one half turn) using a microscope at an oblique angle. Then, the surgical wounds were sutured. Strict aseptic procedures were used during the operation, and penicillin was administered to prevent infection for 5 days after the operation. The animals were given 0.9% saline (5 mL) to prevent dehydration, and housed in standard rat cages at 26°C. After 1 week, the screw was advanced 0.2 mm every week for 4 weeks. The sham operated animals underwent an identical surgical procedure but did not undergo cord compression. Representative pictures of the surgical procedure are shown in [Figure 1](#).

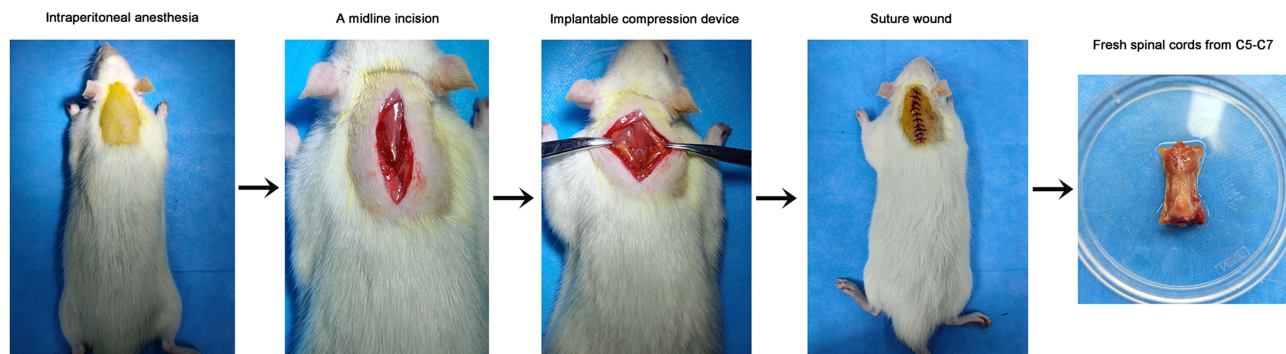


Figure 1 Images of the experimental procedures.

Experimental Design and Groups

Experiment 1

The expression levels of NLPR3 and TNXIP in the anterior horn of the lesion area were measured at 3, 7, 14, and 28 d after chronic cervical cord compression using immunofluorescence. To investigate the expression of TNXIP in the injured spinal cords during progression of CSM, the levels of TNXIP were measured using Western blot. Forty-three rats were used to establish the compression model. Three rats died during surgery.

Experiment 2

Forty rats were blindly and randomly divided the following four groups (n=10): sham group, CSM model group, TNXIP small interfering RNA (siRNA) group and scramble siRNA control group. Two rats died during surgery and were replaced.

In the sham group, rats underwent surgery without compression. In the CSM group, rats underwent surgery with compression. In the scrambled control group, rats were performed surgery with compression, then were intrathecally injected with 20 μ M/day of scrambled siRNA (5'-UUCUCCGAACGUGUCACGdTdT-3' and 5'-ACGUGACACGUUCG GAGAAdTdT-3') in 5 μ L of saline¹⁸ at C5-C6 through catheters for 3 consecutive days. In the TNXIP siRNA group, rats were performed surgery with compression, then were intrathecally injected with 20 μ M/day of TNXIP siRNA (5'-CCAGCC AACUCAAGAGGCAAAGAAAUU-3', and 5'-U UUCUUUGCCUCUUGAGUUGGCUGGUU-3') in 5 μ L of saline at C5-C6 by intrathecal injection¹⁸ for 3 consecutive days.

Behaviors Evaluation

To evaluate behavioral recovery, the 21-point Basso, Beattie and Bresnahan (BBB) locomotor rating scale,²¹ cold allodynia,²² and the inclined plane test²³ were performed 3 days prior to siRNA injection and 0, 3 and 6 days after scramble or TNXIP siRNA injection.

For the BBB locomotor rating scale, joint movements, intervals of uncoordinated stepping, and forelimb and hindlimb coordination were assessed by two examiners independently.

For cold allodynia, a droplet of acetone was placed on the plantar surface of the hind paw of each rat to determine the amount of time (seconds) spent licking, cowering, or shaking the acetone treated hind paw within the next 60 seconds. Acetone was applied twice with an interval of 5 minutes.

For the inclined plane test, rats were placed on a smooth board. The board was initially placed horizontally (0°), and the angle was increased by 5–10° after each attempt. The highest angle the rat could maintain for 8 seconds was recorded.

Samples Collection

After behaviors evaluation, all rats were anesthetized by intraperitoneal injection of pentobarbital (40 mg/kg), and sacrificed by perfusion with 4% paraformaldehyde. Fresh spinal cords from C5-C7 were collected, and some were fixed with 4% paraformaldehyde for overnight, then embedded in paraffin. Others were stored at -80°C .

TdT-Mediated dUTP Nick-End Labeling (TUNEL) Staining

The embedded tissues were cut into 3- μm sections at room temperature, and soaked in xylene twice for 5 mins. After washing with 100% ethanol twice for 5 min, the sections rehydrated in gradient ethanol (95%, 90%, 80%, 70%) for 5min each step. After washing with phosphate buffered saline (PBS), the sections were stained with Coralite[®]488 TUNEL apoptosis detection kit (#PF00006, Proteintech, Wuhan, China) for 2 h at 37°C . The reaction solution was removed, and the sections were washed with PBS twice for 5 min, then washed with buffer containing bovine serum albumin (BSA) for 5 min three times to reduce background. After dehydration, the sections were covered and visualized using a light microscope (DM1000 LED, Leica, Germany).

Immunofluorescence

The embedded sections (3 μm) were placed in 0.1 M sodium citrate buffer for 30 min at 95°C . Then, the sections were blocked with 1% BSA and 0.1% Triton X-100 for 60 min. Rabbit anti-rat NeuN (1:300, 702022, ThermoFisher), TXNIP (1:300, MA5-32771, ThermoFisher), NLRP3 (1:300, MA5-32255, ThermoFisher), and pro-caspase-1 (1:300, MA5-35833, ThermoFisher) antibodies were added, and the sections were incubated overnight at 4°C . The secondary antibody rabbit anti-mouse IgG (H+L) FITC (1:1000, 11-4011-85, ThermoFisher) was added and incubated for 2 h in the dark.

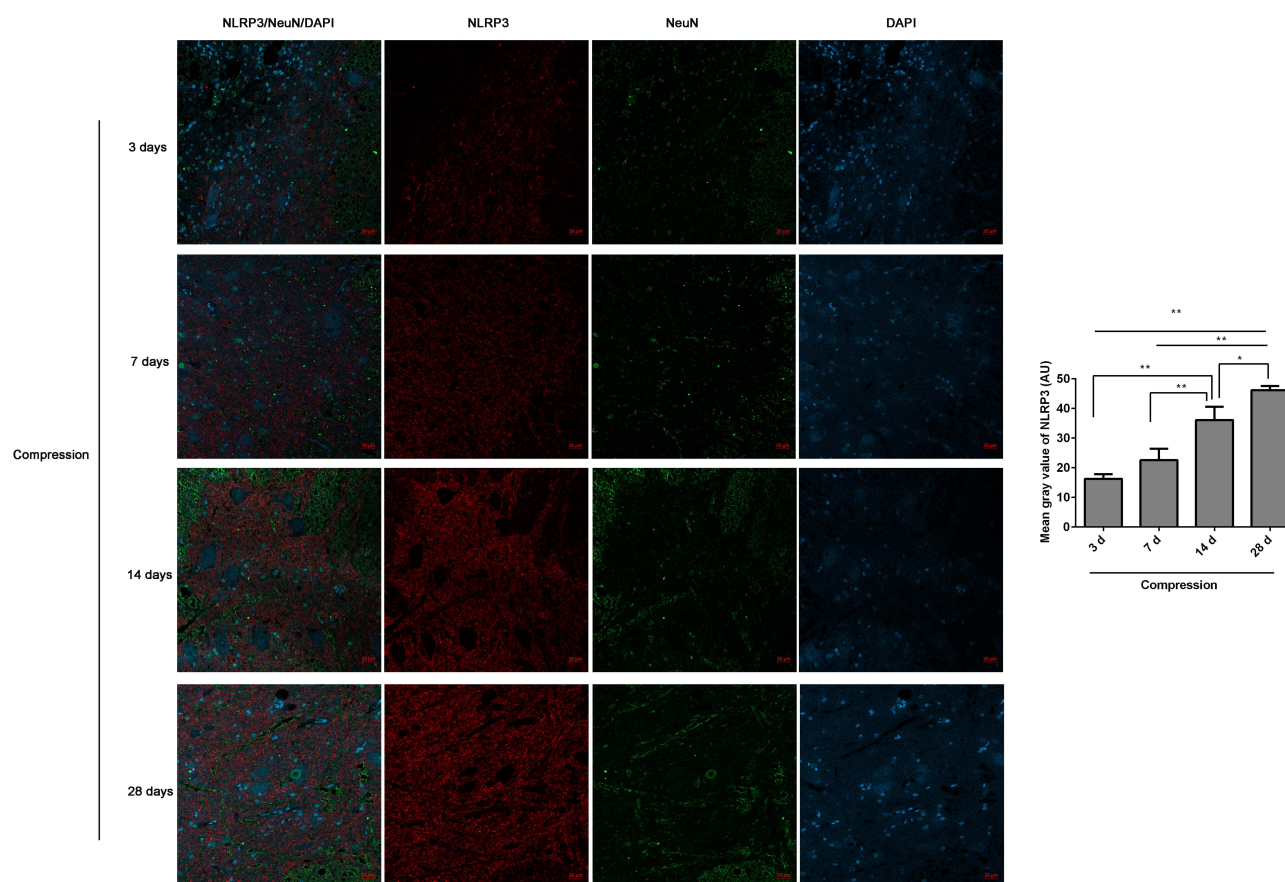


Figure 2 The expression of NLRP3/NeuN in the anterior horn of lesioned spinal cord following compression was analyzed by immunofluorescence. The mean fluorescence intensities of NLRP3 were analyzed by Image J software, and represented as mean gray values. * $P<0.05$, ** $P<0.01$.

Then, the sections were stained with DAPI for 10 min in the dark. The sections were visualized using by laser confocal microscopy (LSM800, Zeiss, Germany) and photographed.

Western Blot

Spinal cord tissues were washed with PBS and homogenized in lysate buffer (Cells-to-C_TTM, 4391851C, ThermoFisher, China) to collect proteins. Proteins (40 µg per lane) were separated using 10% SDS-PAGE (Bio-Rad Laboratories, Inc.) then transferred to PVDF membranes. After blocking for 1 h at room temperature, the membranes were incubated with primary antibodies at 4°C overnight. The primary antibodies included rabbit anti-rat TXNIP (1:800, MA5-32771, ThermoFisher), NLRP3 (1:800, MA5-32255, ThermoFisher), pro-caspase-1 (1:800, MA5-35833, ThermoFisher) and GAPDH (1:10000, PA1-16777, ThermoFisher). After washing with 0.01% Tris buffered saline with Tween-20 every three times for 10 min, the sections were incubated with rabbit anti-goat IgG (H+L) antibody (1:10000, 31402,

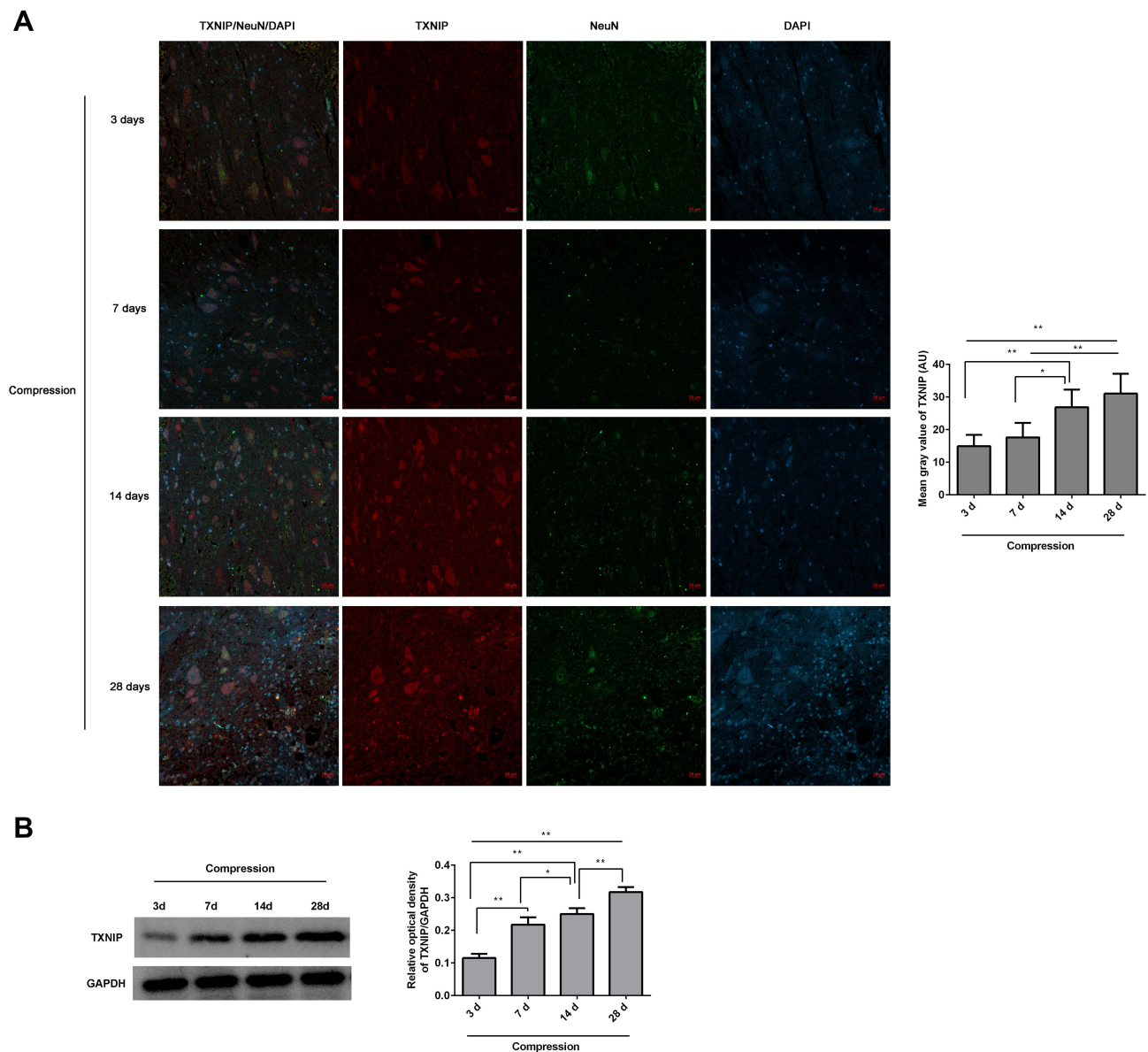


Figure 3 The expression of TXNIP in the lesioned spinal cord following compression was observed. **(A)** The TXNIP/NeuN expression in the anterior horn of lesioned spinal cords was analyzed by immunofluorescence. The mean fluorescence intensities of TXNIP were analyzed by Image J software, and represented as mean gray values. **(B)** The TXNIP expression in the lesioned spinal cords was analyzed by Western blot. The gray values of protein bands were analyzed by Image J software, and protein expression was normalized to GAPDH. * $P < 0.05$, ** $P < 0.01$.

ThermoFisher) at room temperature for 1 h. The protein bands were visualized using Signalfire™ ECL reagent (#6883, Cell Signaling Technology, China).

Statistical Analysis

Image J software (National Institutes of Health, USA) was used to quantify the mean fluorescence intensity of the cells and the gray value of protein bands. SPSS 20.0 statistical analysis software (IBM, Chicago, IL, USA) was used to analyze the data. Results are expressed as the mean \pm standard deviation. One-way analysis of variance was used for data analysis among multiple groups, followed by the LSD test for post hoc analysis. $P < 0.05$ indicated statistically significant differences.

Results

TXNIP and NLRP3 Expression Increased in the Lesioned Area of Spinal Cords Following Progress of CSM

The expression levels of NLRP3/NeuN (Figure 2) and TXNIP/NeuN (Figure 3A) in the anterior horn of lesioned area following cervical cord compression were observed using immunofluorescence. We found that NLRP3 was not expressed in neurons, but TXNIP was expressed in neurons. After compression surgery, the mean gray values of NLRP3 and TXNIP in the anterior horn of damaged spinal cords increased significantly in a time-dependent manner. The mean gray values were significantly higher after 14 days of compression than those after 3 or 7 days of compression. The expression levels of TXNIP in the damaged spinal cords were analyzed using Western blot (Figure 3B). The expression of TXNIP significantly increased following compression in a time-dependent manner.

Inhibition of TXNIP Resulted in Behavioral Improvement in Rats with CSM

To study the effects of TXNIP on behaviors of rat with CSM, TXNIP siRNA and scrambled control were intrathecally injected into C5-C6 spinal cord. Behavior was assessed using BBB scores (Figure 4A), cold allodynia (Figure 4B), and the inclined plane test (Figure 4C). The results showed that the BBB scores (Figure 4A) and highest angle maintained (Figure 4C) were significantly lower in the rats with CSM compared with those in the sham operated rats. After injection

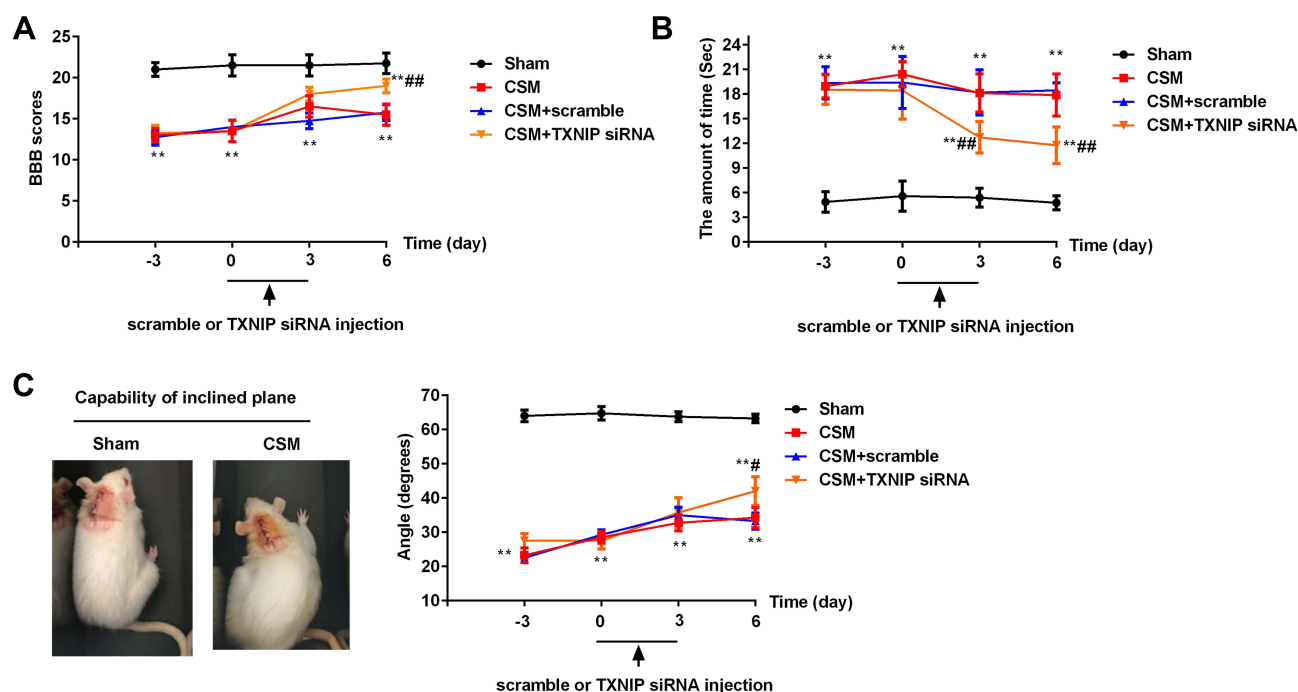


Figure 4 Inhibition of TXNIP improved CSM-induced behavioral deficits. (A) The 21-point Basso, Beattie and Bresnahan (BBB) locomotor rating scale; (B) cold allodynia; (C) inclined plane test. Compared with the sham group, $^{**}P < 0.01$; compared with the scrambled group, $^{#}P < 0.05$, $^{###}P < 0.01$.

of TNXIP siRNA, the BBB scores and highest angle maintained were increased contrasted to the scramble control injection. The CSM group spent more time than the sham-operated group licking the acetone-treated paw (Figure 4B). Injection of TNXIP siRNA significantly reduced time spent licking the acetone treated area compared. No differences in behavioral scores were observed between the CSM group and the scramble group.

Inhibition of TNXIP Suppressed Cell Apoptosis in the Anterior Horn of Lesioned Spinal Cord Following CSM

Apoptosis in the anterior horn of lesioned spinal cord was measured by TUNEL staining (Figure 5). In Figure 5A, it showed the positive control TUNEL control. Black arrows indicate apoptotic cells. Figure 5B shows the results of TUNEL staining in the different groups. Apoptosis was significantly increased in the CSM rats compared with that in the

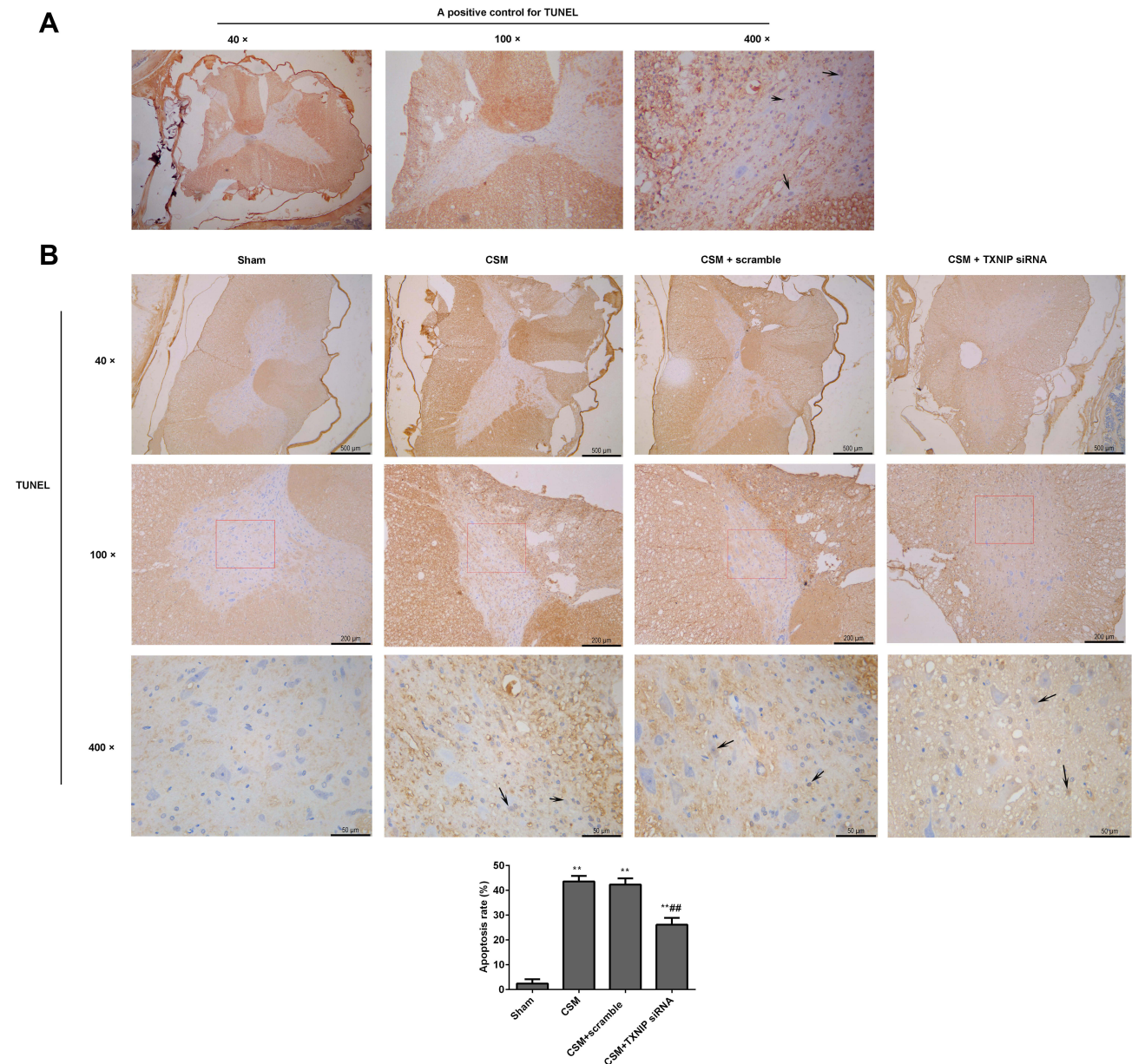


Figure 5 Inhibition of TNXIP reduced apoptosis in the anterior horn of the lesioned area following CSM. **(A)** Positive TUNEL staining control. **(B)** Apoptosis in the anterior horn of the lesioned area was analyzed by TUNEL staining. Black arrows show apoptotic cells. Apoptosis rate (%) = the numbers of apoptosis cells/total numbers of cells $\times 100\%$. The numbers of cells were counted using Image J software. Compared with the sham group, ** $P < 0.01$; compared with the scrambled group, ## $P < 0.01$.

sham rats. After injection of TXNIP siRNA, apoptosis rate in the anterior horn of lesion area was obviously reduced compared with that in the scrambled control group.

Inhibition of TXNIP Reduced Activation of NLRP3 in the Anterior Horn of Lesioned Spinal Cord Following CSM

The fluorescence intensities of TXNIP/NeuN (Figure 6) and NLRP3/NeuN (Figure 7) in the anterior horn of the lesioned area were analyzed by immunofluorescence. The mean gray values of TXNIP and NLRP3 were significantly higher in the CSM rats than those in the sham rats. After injection of scrambled siRNA, the mean gray areas of TXNIP and NLRP3 did not differ from those in the CSM group. In contrast, the mean gray values were significantly decreased in CSM rats following injection of TXNIP siRNA compared with those in the scrambled control group.

Inhibition of TXNIP Reduced NLRP3 Mediated Recruitment of Pro-Caspase-1 in the Anterior Horn of Lesioned Spinal Cord Following CSM

The fluorescence intensities of pro-caspase-1/NeuN in the anterior horn of the lesioned area were analyzed by immunofluorescence (Figure 8A). It showed that pro-caspase-1 was expressed in neurons. The mean gray values of pro-caspase-1 in the CSM rats were significantly increased by contrast to those in the sham rats. Treatment with TXNIP siRNA significantly reduced the fluorescence intensity of pro-caspase-1 in the CSM rats compared with that in the scrambled group.

Additionally, the expression levels of TXNIP, NLRP3 and pro-caspase-1 in the lesioned spinal cords were analyzed by Western blot (Figure 8B). The relative expression levels of these proteins were normalized to GAPDH. After surgical

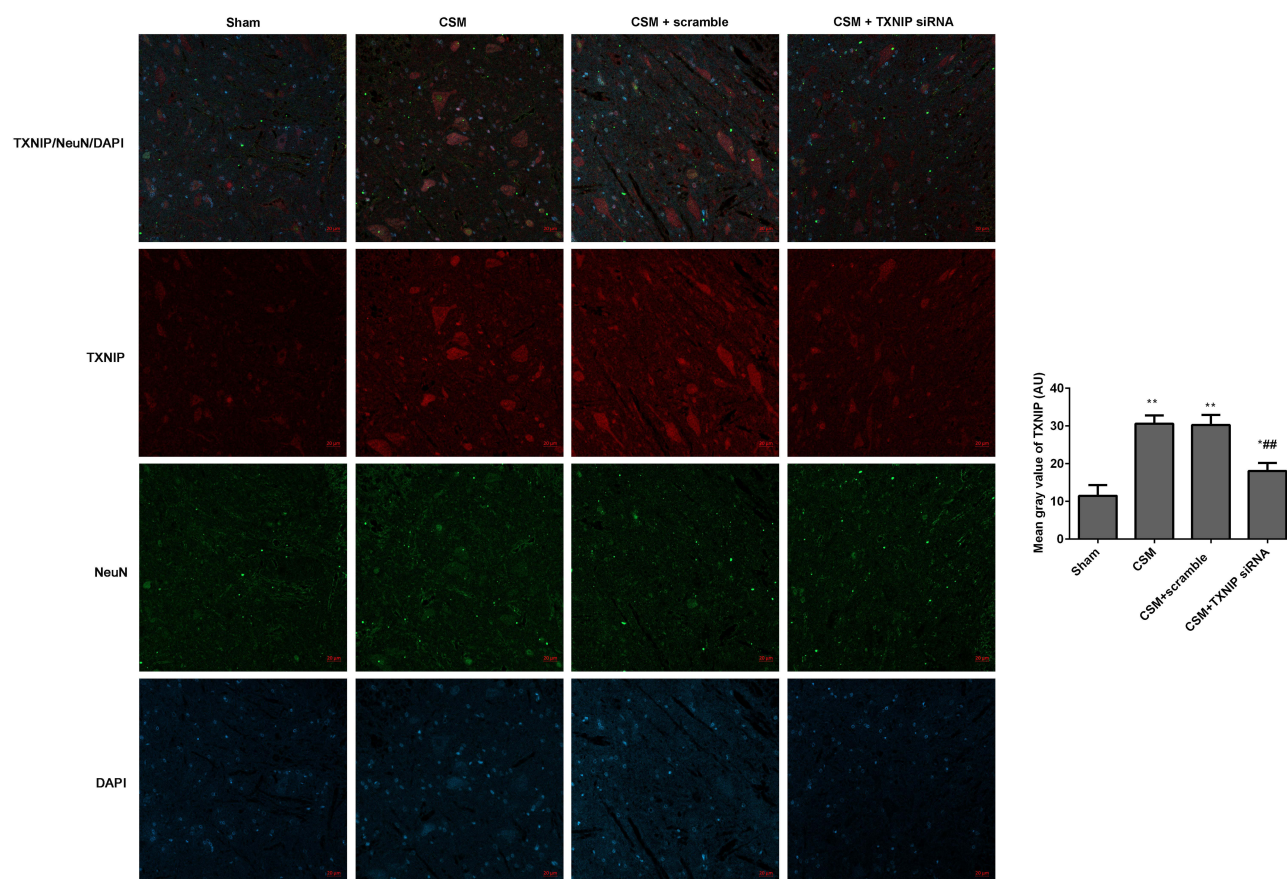


Figure 6 Inhibition of TXNIP declined the TXNIP expression in the anterior horn of the lesioned area following CSM. The mean fluorescence intensities of TXNIP/NeuN were analyzed by immunofluorescence. The mean gray values were analyzed using Image J software. Compared with the sham group, * $P < 0.05$, ** $P < 0.01$; compared with the scrambled group, ## $P < 0.01$.

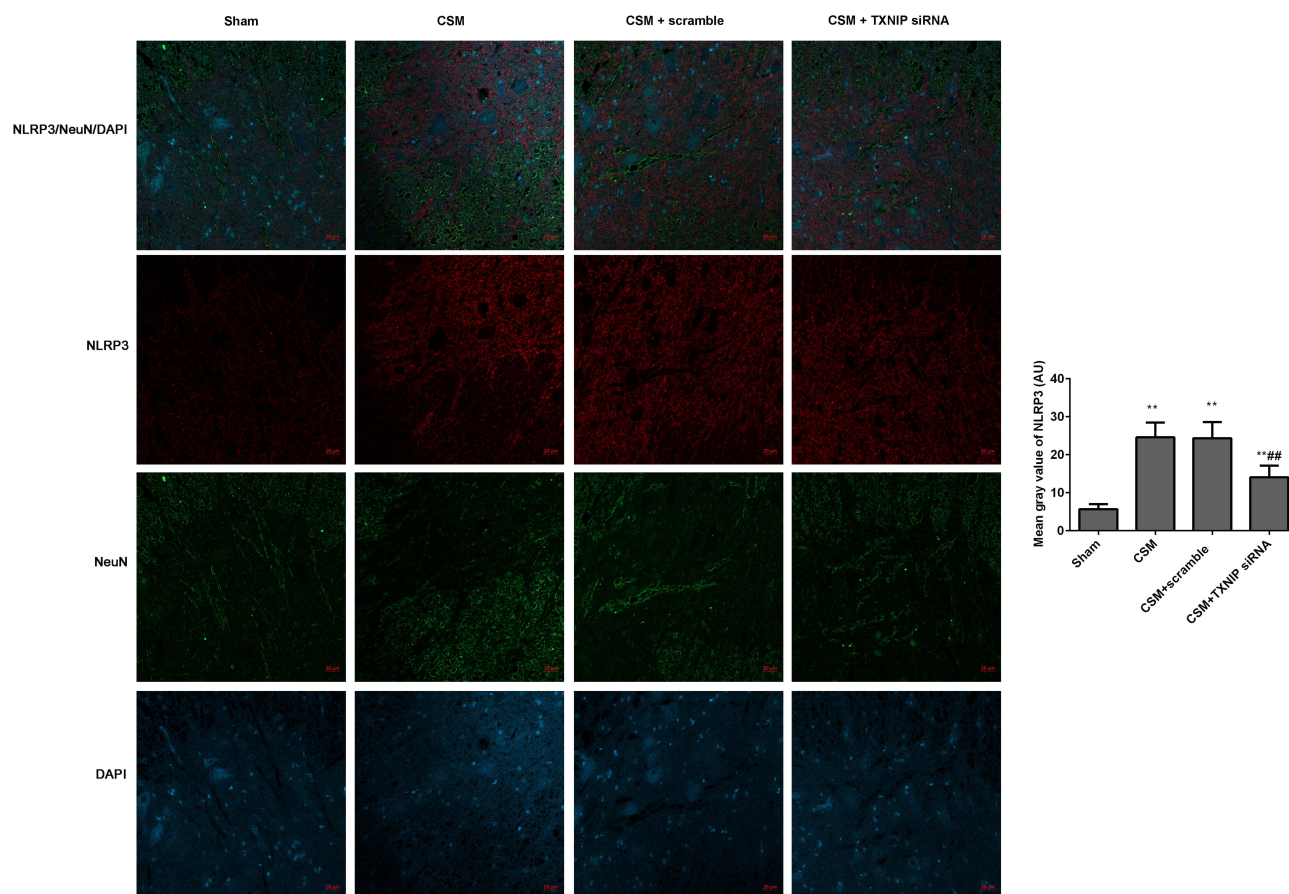


Figure 7 Inhibition of TXNIP declined the NLRP3 expression in the anterior horn of the lesioned area following CSM. The mean fluorescence intensities of NLRP3/NeuN were analyzed by immunofluorescence. The mean gray values were analyzed by Image J software. Compared with the sham group, ** $P < 0.01$; compared with the scrambled group, *** $P < 0.01$.

compression, the levels of TXNIP, NLRP3 and pro-caspase-1 were clearly increased in the lesioned spinal cords contrasted to those in the sham rats. There was no significant difference between the CSM group and scramble group. Injection with TXNIP siRNA significantly reduced the expression of TXNIP, NLRP3, and pro-caspase-1.

Discussion

Thioredoxin-interacting protein is an endogenous scavenger of reactive oxygen species widely expressed in variety of cells and regulates the energy metabolism by acting as a molecular sensor of oxidative stress and inflammation.^{14,24} Studies have shown the TXNIP/NLRP3 axis is involved in the spinal cord injury,¹⁷ including chronic constriction injury^{19,25} and partial sciatic nerve ligation induced sciatic nerve injury.¹⁸ However, no studies have focused on the role of the TXNIP/NLRP3 axis in CSM. In this study, we found that TXNIP expression was increased in the lesioned spinal cord following CSM. Furthermore, NLRP3 expression increased in the damaged anterior horn during progression of CSM in a time-dependent manner. In addition, we found that TXNIP was expressed in neurons, but NLRP3 was not expressed in neurons, which was consistent with previous studies.^{1,18} Although TXNIP and NLRP3 expression levels were enhanced in response to CSM, the role of TXNIP in activation of the NLRP3 inflammasome in CSM required further characterization.

To test our hypothesis that inhibition of TXNIP could reduce NLRP3 inflammasome activation in CSM, TXNIP siRNA or scrambled siRNA was injected into spinal cords. Behavioral evaluation using BBB scores, cold allodynia and the inclined plane test showed that inhibition of TXNIP improved behavioral parameters of rats with CSM, and suppressed apoptosis in the damaged anterior horn. These data showed that inhibition of TXNIP could improve motor

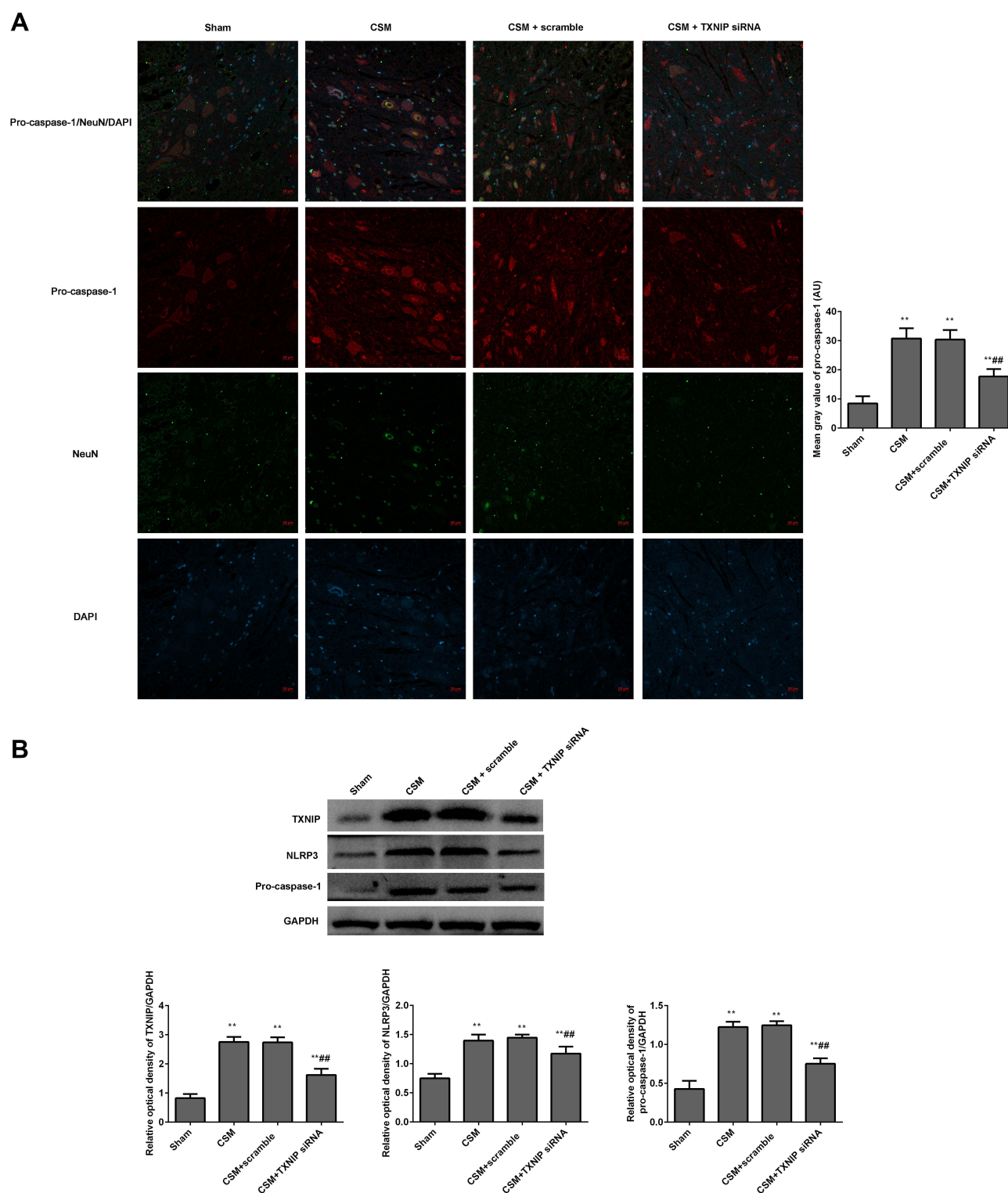


Figure 8 Inhibition TXNIP declined the NLRP3 mediated pro-caspase-I expression in the anterior horn of the lesioned area following CSM. **(A)** The mean fluorescence intensities of pro-caspase-I/NeuN were analyzed by immunofluorescence. **(B)** The expression levels of TXNIP, NLRP3 and pro-caspase-I in the lesioned spinal cords were measured by Western blot. The mean grays were analyzed by the Image J software. Compared with the sham group, ** $P < 0.01$; compared with the scrambled group, ## $P < 0.01$.

function recovery, which indicated that TNXIP might be a therapeutic target for improving CSM. Our data would play an important role in finding suitable therapeutic drugs or developing corresponding targeted drugs for improving CSM in the future.

Neuroinflammation is a critical mechanism of CSM-related damage through breakdown of the blood-spinal cord barrier and distortion of the local microvasculature.^{1,26} As is well known, neuroinflammation is strongly associated with activation of the NLRP3 inflammasome.^{7,11,13,27} The classical pyroptosis pathway involves formation of the NLRP3 inflammasome, which is comprised of NLRP3, ASC, and pro-caspase-1. After activation, NLRP3 recruits ASC protein, which then recruits the pro-caspase-1 and promotes cleavage to caspase-1, resulting in production and secretion of inflammatory cytokines.^{13,28} Rat models of CSM have shown that the NLRP3 inflammasome was activated in damaged spinal cord.^{1,4} However, the mechanisms by which the NLRP3 inflammasome mediate damage in CSM are not clear. We found that inhibition of TNXIP significantly reduced expression of NLRP3 and pro-caspase-1 in the damaged spinal cord of rats with CSM. As known, TRX binds to TNXIP and inhibits its activity under physiological conditions.²⁹ However, in some pathological conditions, excessive ROS promotes dissociation of TNXIP from TRX, and free TNXIP binds to NLRP3, resulting in NLRP3 inflammasome activation and activation of the inflammatory response.^{18,29} In this study, pro-caspase-1 was expressed in neurons of damaged spinal cord, which indicated that TNXIP-mediated activation of the NLRP3 inflammasome participated in neuronal apoptosis. These results confirmed our hypothesis that the TNXIP/NLRP3 axis is an effector of damage in spinal cords in a rat model of CSM. The TNXIP/NLRP3 axis may be a target for improving CSM in the future.

Further study of the role of TNXIP in CSM is needed. Forkhead box O1 transcriptional factor (FoxO1)³⁰ and nuclear factor-erythroid 2-related factor 2 (Nrf2)³¹ have shown to regulate TNXIP expression. Furthermore, TNXIP has been shown to interact with other proteins besides NLRP3, such as importin- α ³² and human ecdysoneless (hEcd).³³ These findings indicated that TNXIP might be an important hub coordinator of different pathological processes in CSM.

Conclusions

Our findings showed that TNXIP participated in CSM progression in rats through activation of NLRP3, and subsequent induction of neuroinflammation and apoptosis in damaged spinal cords. Inhibition of TNXIP suppressed activation of the NLRP3 inflammasome in CSM spinal cords, which suggested that TNXIP might be a potential therapeutic strategy to prevent NLRP3-mediated inflammation in CSM.

Data Sharing Statement

All data generated or analyzed during this study are available from the corresponding author upon reasonable request.

Ethics Approval

All experimental protocols of this study were approved by the Animal Care Committee of the Yantaishan Hospital (Number: 2021002), and followed the Guide for the Care and Use of Laboratory Animals published by the US National Institutes of Health (2011).

Author Contributions

All authors made a significant contribution to the work reported, whether that is in the conception, study design, execution, acquisition of data, analysis and interpretation, or in all these areas; took part in drafting, revising or critically reviewing the article; gave final approval of the version to be published; have agreed on the journal to which the article has been submitted; and agree to be accountable for all aspects of the work.

Funding

There is no funding to report.

Disclosure

The authors declare that there is no conflict of interest.

References

1. Zhou LY, Yao M, Tian ZR, et al. Muscone suppresses inflammatory responses and neuronal damage in a rat model of cervical spondylotic myelopathy by regulating Drp1-dependent mitochondrial fission. *J Neurochem*. 2020;155(2):154–176. doi:10.1111/jnc.15011.
2. McCormick JR, Sama AJ, Schiller NC, Butler AJ, Donnelly CJ 3rd. Cervical spondylotic myelopathy: a guide to diagnosis and management. *J Am Board Fam Med*. 2020;33(2):303–313. doi:10.3122/jabfm.2020.02.190195.
3. Dhillon RS, Parker J, Syed YA, et al. Axonal plasticity underpins the functional recovery following surgical decompression in a rat model of cervical spondylotic myelopathy. *Acta Neuropathol Commun*. 2016;4(1):89. doi:10.1186/s40478-016-0359-7.
4. Zhou L, Yao M, Tian Z, et al. Echinacoside attenuates inflammatory response in a rat model of cervical spondylotic myelopathy via inhibition of excessive mitochondrial fission. *Free Radic Biol Med*. 2020;152:697–714. doi:10.1016/j.freeradbiomed.2020.01.014.
5. Moon ES, Karadimas SK, Yu WR, Austin JW, Fehlings MG. Riluzole attenuates neuropathic pain and enhances functional recovery in a rodent model of cervical spondylotic myelopathy. *Neurobiol Dis*. 2014;62:394–406. doi:10.1016/j.nbd.2013.10.020.
6. Isobe T, Yaguchi H, Matsui K, Inoue K. [A case of cervical spondylotic amyotrophy resembling post-polio syndrome]. 1例の脊髄灰白質炎後症候群に類似した頸椎性筋萎縮. *Rinsho Shinkeigaku*. 2006;46(1):59–61. Japanese.
7. Mortezaee K, Khanlarkhani N, Beyer C, Zendedel A. Inflammasome: its role in traumatic brain and spinal cord injury. *J Cell Physiol*. 2018;233(7):5160–5169. doi:10.1002/jcp.26287.
8. Li Y, Ritzel RM, Khan N, et al. Delayed microglial depletion after spinal cord injury reduces chronic inflammation and neurodegeneration in the brain and improves neurological recovery in male mice. *Theranostics*. 2020;10(25):11376–11403. doi:10.7150/thno.49199.
9. Pfyffer D, Wyss PO, Huber E, et al. Metabolites of neuroinflammation relate to neuropathic pain after spinal cord injury. *Neurology*. 2020;95(7):e805–e814. doi:10.1212/wnl.00000000000010003.
10. Brockie S, Hong J, Fehlings MG. The role of microglia in modulating neuroinflammation after spinal cord injury. *Int J Mol Sci*. 2021;22(18). doi:10.3390/ijms22189706.
11. Swanson KV, Deng M, Ting JP. The NLRP3 inflammasome: molecular activation and regulation to therapeutics. *Nat Rev Immunol*. 2019;19(8):477–489. doi:10.1038/s41577-019-0165-0.
12. Gaidt MM, Hornung V. The NLRP3 inflammasome renders cell death pro-inflammatory. *J Mol Biol*. 2018;430(2):133–141. doi:10.1016/j.jmb.2017.11.013.
13. Al Mamun A, Wu Y, Monalisa I, et al. Role of pyroptosis in spinal cord injury and its therapeutic implications. *J Adv Res*. 2021;28:97–109. doi:10.1016/j.jare.2020.08.004.
14. Tsubaki H, Tooyama I, Walker DG. Thioredoxin-interacting protein (TXNIP) with focus on brain and neurodegenerative diseases. *Int J Mol Sci*. 2020;21(24). doi:10.3390/ijms21249357.
15. Pan M, Zhang F, Qu K, Liu C, Zhang J. TXNIP: a double-edged sword in disease and therapeutic outlook. *Oxid Med Cell Longev*. 2022;2022:7805115. doi:10.1155/2022/7805115.
16. Yu P, Zhang X, Liu N, et al. Pyroptosis: mechanisms and diseases. *Signal Transduct Target Ther*. 2021;6(1):128. doi:10.1038/s41392-021-00507-5.
17. Ren Z, Liang W, Sheng J, et al. Gal-3 is a potential biomarker for spinal cord injury and Gal-3 deficiency attenuates neuroinflammation through ROS/TXNIP/NLRP3 signaling pathway. *Biosci Rep*. 2019;39(12). doi:10.1042/bsr20192368.
18. Pan Z, Shan Q, Gu P, et al. miRNA-23a/CXCR4 regulates neuropathic pain via directly targeting TXNIP/NLRP3 inflammasome axis. *J Neuroinflammation*. 2018;15(1):29. doi:10.1186/s12974-018-1073-0.
19. Hu T, Sun Q, Gou Y, et al. Salidroside alleviates chronic constriction injury-induced neuropathic pain and inhibits of TXNIP/NLRP3 pathway. *Neurochem Res*. 2021. doi:10.1007/s11064-021-03459-y.
20. Vidal PM, Ulfendrup A, Badner A, Hong J, Fehlings MG. Methylprednisolone treatment enhances early recovery following surgical decompression for degenerative cervical myelopathy without compromise to the systemic immune system. *J Neuroinflammation*. 2018;15(1):222. doi:10.1186/s12974-018-1257-7.
21. Basso DM, Beattie MS, Bresnahan JC. A sensitive and reliable locomotor rating scale for open field testing in rats. *J Neurotrauma*. 1995;12(1):1–21. doi:10.1089/neu.1995.12.1.
22. Chung D, Cho DC, Park SH, et al. Cold allodynia after C2 root resection in Sprague-Dawley rats. *J Korean Neurosurg Soc*. 2018;61(2):186–193. doi:10.3340/jkns.2017.0404.019.
23. Rivlin AS, Tator CH. Effect of duration of acute spinal cord compression in a new acute cord injury model in the rat. *Surg Neurol*. 1978;10(1):38–43.
24. Zhou R, Tardivel A, Thorens B, Choi I, Tschopp J. Thioredoxin-interacting protein links oxidative stress to inflammasome activation. *Nat Immunol*. 2010;11(2):136–140. doi:10.1038/ni.1831.
25. Miao J, Zhou X, Ji T, Chen G. NF- κ B p65-dependent transcriptional regulation of histone deacetylase 2 contributes to the chronic constriction injury-induced neuropathic pain via the microRNA-183/TXNIP/NLRP3 axis. *J Neuroinflammation*. 2020;17(1):225. doi:10.1186/s12974-020-01901-6.
26. Kurokawa R, Murata H, Ogino M, Ueki K, Kim P. Altered blood flow distribution in the rat spinal cord under chronic compression. *Spine*. 2011;36(13):1006–1009. doi:10.1097/BRS.0b013e3181eaf33d.
27. Zhou Z, He M, Zhao Q, et al. Panax notoginseng saponins attenuate neuroinflammation through TXNIP-mediated NLRP3 inflammasome activation in aging rats. *Curr Pharm Biotechnol*. 2021;22(10):1369–1379. doi:10.2174/1389201021999201110204735.
28. Zahid A, Li B, Kombe AJK, Jin T, Tao J. Pharmacological inhibitors of the NLRP3 inflammasome. *Front Immunol*. 2019;10:2538. doi:10.3389/fimmu.2019.02538.
29. Li N, Zhao T, Cao Y, et al. Tangshen formula attenuates diabetic kidney injury by imparting anti-pyroptotic effects via the TXNIP-NLRP3-GSDMD axis. *Front Pharmacol*. 2020;11:623489. doi:10.3389/fphar.2020.623489.
30. Ji L, Wang Q, Huang F, et al. FOXO1 overexpression attenuates tubulointerstitial fibrosis and apoptosis in diabetic kidneys by ameliorating oxidative injury via TXNIP-TRX. *Oxid Med Cell Longev*. 2019;2019:3286928. doi:10.1155/2019/3286928.
31. Lv H, Zhu C, Wei W, et al. Enhanced Keap1-Nrf2/Trx-1 axis by daphnetin protects against oxidative stress-driven hepatotoxicity via inhibiting ASK1/JNK and TxnIP/NLRP3 inflammasome activation. *Phytomedicine*. 2020;71:153241. doi:10.1016/j.phymed.2020.153241.

32. Nishinaka Y, Masutani H, Oka S, et al. Importin alpha1 (Rch1) mediates nuclear translocation of thioredoxin-binding protein-2/vitamin D(3)-up-regulated protein 1. *J Biol Chem*. 2004;279(36):37559–37565. doi:10.1074/jbc.M405473200
33. Suh HW, Yun S, Song H, et al. TXNIP interacts with hEcd to increase p53 stability and activity. *Biochem Biophys Res Commun*. 2013;438(2):264–269. doi:10.1016/j.bbrc.2013.07.036

Journal of Inflammation Research

Dovepress

Publish your work in this journal

The Journal of Inflammation Research is an international, peer-reviewed open-access journal that welcomes laboratory and clinical findings on the molecular basis, cell biology and pharmacology of inflammation including original research, reviews, symposium reports, hypothesis formation and commentaries on: acute/chronic inflammation; mediators of inflammation; cellular processes; molecular mechanisms; pharmacology and novel anti-inflammatory drugs; clinical conditions involving inflammation. The manuscript management system is completely online and includes a very quick and fair peer-review system. Visit <http://www.dovepress.com/testimonials.php> to read real quotes from published authors.

Submit your manuscript here: <https://www.dovepress.com/journal-of-inflammation-research-journal>